Low-Temperature IR and NMR Studies of the Interaction of Group 8 Metal Dihydrides with Alcohols

Evgenii I. Gutsul,[b] Natalia V. Belkova,[b] Maria S. Sverdlov,[b] Lina M. Epstein,*[b] Elena S. Shubina,*[b] Vladimir I. Bakhmutov,*[c] Tatiana N. Gribanova,[d] Ruslan M. Minyaev,*[d] Claudio Bianchini,*[a] Maurizio Peruzzini,*[a] and Fabrizio Zanobini[a]

Abstract: The reactions of the octahedral dihydrido complexes $[MH_2(PP_3)]$ [M = Fe, Ru, Os; PP_3=P-$(CH_2CH_2PPh_2)_3$] with a variety of weak ROH acids have been studied by IR and NMR methods in either CH_2Cl_2 or THF in the temperature range from 190 to 290 K. This study has allowed the determination of the spectral and thermodynamic properties associated with the formation of dihydrogen bonds (DHB) between the terminal hydrides and the OH group. Both the DHB enthalpy values and the hydride basicity factors (E_j) have been found to increase in the order Fe < Ru < Os. The proton transfer process, leading to the DHB complexes, and eventually to η^2-H_2 products, has been found to depend on the acidic strength of the alcohol as well as the nature of the solvent. Low temperature IR and NMR techniques have been used to trace the complete energy profile of the proton transfer process involving the osmium complex $[OsH_2(PP_3)]$ with trifluoroethanol.

Keywords: hydrides · hydrogen bonding · IR spectroscopy · polyphosphines · theoretical methods

Introduction

Unconventional dihydrogen bonding (DHB) represents a new type of organizing interaction of much current interest in organometallic chemistry, homogeneous and heterogeneous catalysis as well as biochemistry.[1]

DHB–metal complexes are usually generated by reaction of compounds containing terminal hydride ligands with Brønsted acids.[2, 3] Studies of these reactions in low polarity solvents have been carried out and have provided thermodynamic data associated with the stability of the resultant DHB compounds.[1d, 2d, e, 3a, b] A question that still needs to be addressed regards the influence of the hydride-supporting metal on the formation and stability of the DHB interaction; in particular no thermodynamic data correlating the DHB strength and the position of the metal in the Periodic Table has been yet provided.

Aimed at filling this gap, we decided to examine the reactions of the classical dihydride complexes $[MH_2(PP_3)]$ [M = Fe, (**1**); Ru, (**2**); Os (**3**); PP_3=$P(CH_2CH_2PPh_2)_3$] with weak acids of the type ROH. Indeed, these Group 8 dihydrides constitute a family of octahedral transition-metal complexes sharing an identical ligand environment as well as reactivity towards Brønsted acids.[4] The latter can transform the dihydrides into cationic dihydrogen complexes $[M(H)(H_2)(PP_3)]X$ with no change of the metal oxidation state [M = Fe, (**4**); Ru, (**5**); Os (**6**); X = non-coordinating counter-anion] (Scheme 1).[4a–e]

In this paper, we report a study of the spectral (IR, ^{1}H NMR) and thermodynamic properties of several DHB compounds of the type MH···HX obtained by treatment of **1**–**3** with alcohols in different solvents. IR and NMR measurements have been carried out at low temperature to shift the solution equilibrium towards the formation of the DHB adducts and to minimise undesirable processes (e.g.,

[a] Dr. C. Bianchini, Dr. M. Peruzzini, F. Zanobini
Istituto di Chimica dei Composti Organometallici
ICCOM-CNR, Via J. Nardi 39
50132 Firenze (Italy)
E-mail: bianchin@fi.cnr.it, peruz@fi.cnr.it

[b] Prof. L. M. Epstein, Prof. E. S. Shubina, Dipl.-Chem. E. I. Gutsul, Dr. N. V. Belkova, Dipl.-Chem. M. S. Sverdlov
A.N. Nesmeyanov Institute of Organoelement Compounds
Russian Academy of Sciences
Vavilov str. 28, 119991 Moscow (Russia)
E-mail: epst@ineos.ac.ru, shu@ineos.ac.ru

[c] Prof. V. I. Bakhmutov
Department of Chemistry
Texas A&M University
PO Box 30012, College Station TX 77842-3012 (USA)
E-mail: bakhmoutov@mail.chem.tamu.edu

[d] Prof. R. M. Minyaev, Dr. T. N. Gribanova
Institute of Physical and Organic Chemistry
Rostov State University
194/2 Stachka Ave., 344090 Rostov-on-Don (Russia)
E-mail: minyaev@ipoc.rsu.ru

 DOI: 10.1002/chem.200204510

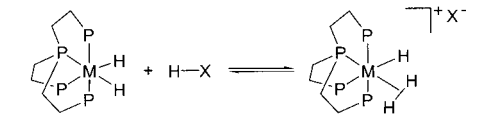

M = Fe (**1**), Ru (**2**), Os (**3**) M = Fe (**4**), Ru (**5**), Os (**6**)

X = OSO_2CF_3, BF_4

Scheme 1. Reversible protonation of $[MH_2(PP_3)]$.

hydride–chlorine exchange) and decomposition pathway. These techniques have been used to trace the complete energy profile of the proton transfer process involving the osmium complex $[OsH_2(PP_3)]$ and trifluoroethanol.

Results and Discussion

Hydrogen bonding between the dihydrides $[MH_2(PP_3)]$ and various alcohols

IR Analysis of the ν_{OH} region: The formation of hydrogen bonds between the dihydrides $[MH_2(PP_3)]$ and alcohols was primarily established by an IR study in the ν_{OH} region.[1d, 3a, b] The IR spectra of the metal dihydrides **1**–**3**, dissolved in CH_2Cl_2, were recorded in the presence of alcohols exhibiting rather different pK_a values [methanol (MeOH), 2-propanol (*i*PrOH), 2-fluoroethanol (MFE), 2,2,2-trifluoroethanol (TFE), hexafluoro-2-propanol (HFIP) and perfluoro-*tert*-butanol (PFTB)]. To exclude the occurrence of self-association phenomena, the concentration of the proton donor was varied between 0.005 and 0.01M. Under these conditions, the observed decrease in intensity (A) of the $\nu_{OH(free)}$ band of the alcohol and the appearance of a low-frequency shifted broad ν_{OH} band confirmed unequivocally the formation of the DHB species $[MH_2(PP_3)]\cdots HOR$.[1f]

As reported in Table 1, the low-frequency shift $[\Delta\nu_{OH} = \nu_{OH(free)} - \nu_{OH(bonded)}]$ was found to increase with the strength of the proton donor.

Table 1. IR spectral characteristics of the hydrogen-bonded adducts $[(PP_3)MH_2\cdots HOR]$ in CH_2Cl_2.

Hydride	Alcohol	$\nu_{(OH)free}$	$\nu_{(OH)bonded}$	$\Delta\nu_{(OH)}$
$[(PP_3)FeH_2]$ (**1**)	MeOH	3624	3462	162
	MFE	3608	3416	192
	TFE	3600	3362	238
$[(PP_3)RuH_2]$ (**2**)	*i*PrOH	3610	3433	177
	TFE	3600	3288	312
	HFIP	3574	3176	398
$[(PP_3)OsH_2]$ (**3**)	MeOH	3624	3364	260
	MFE	3608	3262	346
	TFE	3600	3172	428

The $[MH_2(PP_3)]$ complexes contain three potential hydrogen-bond acceptors: the two chemically inequivalent hydride ligands and the metal(II) centre.[3e] It has been previously established, in fact, that relatively electron-rich metals, such as ruthenium(II), osmium(II) and rhenium(I), can use their d-electron density to form M···HO bonds with alcohols.[1b,h] In our case, unambiguous discrimination between the M-OH···HOR and M···HO bonding modes was achieved by IR and ^{1}H NMR methods (see below).[1f, 2c–e]

IR and Raman assignment of the ν_{MH} bands in 1–3: The solid-state IR spectra of **1**–**3** showed two intense ν_{MH} absorptions in the region between 1950 and 1730 cm^{-1}.[4a–e] Similar bands were found in the IR spectra recorded in either CH_2Cl_2 or THF solution (Table 2).

Based on the symmetry of the dihydrides **1**–**3**, these two bands were initially attributed to symmetric (ν^{s}_{MH}) and asymmetric (ν^{as}_{MH}) M–H stretching vibrations. However, an inspection of the literature data available for dihydride metal complexes revealed that the appearance of two "hydride" bands with similar intensities at remarkably different wavenumbers (frequency difference 120–175 cm^{-1}) is quite uncommon.[5] A variety of rhenium, molybdenum and tungsten

Table 2. IR ν_{MH} absorptions in CH_2Cl_2 and in the solid state (nujol mull).[4]

Hydride	ν^1_{MH}	ν^2_{MH}	$\Delta\nu$[a]
$[FeH_2(PP_3)]$ (**1**)	1854	1730	124
	1856[4]	*1734*	*122*
$[RuH_2(PP_3)]$ (**2**)	1874	1699	175
	1864[4c]	*1722*	*142*
$[OsH_2(PP_3)]$ (**3**)	1950	1810	140
	1942[4d]	*1827*	*115*

[a] $\Delta\nu = \nu^1_{MH} - \nu^2_{MH}$.

Abstract in Italian: *La reazione dei diidruri terminali a geometria ottaedrica $[MH_2(PP_3)]$ [M = Fe, Ru, Os; PP_3=$P(CH_2CH_2PPh_2)_3$] con una varietà di acidi deboli, ROH, è stata studiata mediante spettroscopia IR ed NMR in CH_2Cl_2 o THF nell'intervallo di temperatura tra 190 e 290 K. Tale studio ha permesso di determinare le proprietà spettrali e termodinamiche associate alla formazione del legame ad idrogeno (DHB) tra gli idruri terminali ed il gruppo OH dell'alcole impiegato. Sia i valori dell'entalpia di legame per il DHB che il fattore di basicità dell'idruro (E_j) sono stati definiti dimostrando che essi variano nell'ordine Fe < Ru < Os. Il processo di trasferimento protonico, che dà origine inizialmente ai complessi DHB e successivamente ai corrispondenti idruri non classici, dipende sia dall'acidità dell'alcole che dalla natura del solvente. Il profilo energetico del processo di trasferimento protonico tra l'idruro $[OsH_2(PP_3)]$ e il trifluoroetanolo è stato completamente determinato mediante tecniche spettroscopiche IR ed NMR a bassa temperatura.*

Abstract in Russian:

Реакции октаэдрических дигидридных комплексов $[MH_2(PP_3)]$ [M = Fe, Ru, Os; PP_3 = $P(CH_2CH_2PPh_2)_3$] с различными слабыми ROH кислотами была изучена методами ИК и ЯМР в CH_2Cl_2 или ТГФ в области температур от 190 до 290 К. Это исследование позволило определить спектральные и термодинамические свойства, связанные с образованием диводородных связей (ДВС) между концевыми гидридами и ОН-группой. Установлено, что как величины энтальпии ДВС, так и факторы основности (E_j) возрастают в ряду Fe < Ru < Os. Показано, что процесс перехода протона, ведущий к ДВС комплексам, и, в конечном счете, к η^2-H_2-продукту зависит как от кислотной силы спирта, так и от природы растворителя. Низкотемпературная ИК и ЯМР техника использовалась, чтобы определить энергетический профиль процесса полного перехода протона от трифторэтанола к $[OsH_2(PP_3)]$.

dihydrides exhibit only the symmetric M–H stretching vibration as a broad and weak band.[2d,e, 5a] Also, ab initio quantum mechanical calculations predict that the two absorptions of the MH_2 moiety in the model polyhydrides MH_2, $[MH_2(H_2)]$ and MH_4 (M = Ti, V and Cr) fall at the same wavenumber with the intensity of the ν^{as}_{MH} band significantly higher than that of the ν^{s}_{MH} band.[5b]

In order to overcome these inconsistencies and provide a correct assignment to the hydride absorptions in **1**–**3**, we decided to carry out Raman depolarization measurements of the ν_{MH} lines for the osmium dihydride **3** in CH_2Cl_2 solution. The positions of the Raman and IR bands in **3** were identical to each other and the depolarization ratio, ρ, showed that both lines were strongly and similarly polarized ($\rho = 0.16-0.17$), hence, it was concluded that the observed bands can be unambiguously assigned to the M–H stretching symmetrical modes (A_1).

Since the ν_{MH} frequency may be influenced by the electron-donor properties of the donor group *trans* to the hydride, it was reasonable to associate the lower-frequency ν^{2}_{MH} band to the hydride ligand *trans* to the bridgehead phosphorus atom (P_{apical}), which exerts a stronger *trans*-influence than the terminal phosphorus atoms.[6] It is well known, in fact, that ligands with strong *trans*-influence may cause a low-frequency shift of the IR absorption as a consequence of decreased $M-H^{ax}$ force constant and bond strength.[1e] In conclusion, the ν^{1}_{MH} and ν^{2}_{MH} bands in the hydrides **1**–**3** can be unequivocally assigned to the stretching vibrations of the equatorial (*cis* to P_{apical}) and axial (*trans* to P_{apical}) M–H bonds, respectively, and, therefore, will be referred to as ν^{eq}_{MH} and ν^{ax}_{MH} in forthcoming pages. A theoretical analysis, outlined below, confirms further on this assignment.

IR monitoring of the reactions of 1–3 with alcohols: The addition of MFE, TFE, HFIP or PFTB to CH_2Cl_2 solutions of **1**–**3** caused significant changes in the IR spectra. As an example, Figure 1 shows the IR changes relative to the reactions of **1**–**3** with MFE. Irrespective of the metal complex, the high-frequency band (ν^{eq}_{MH}) shifted to lower frequencies when an excess of MFE was added, while the ν^{ax}_{MH} bands slightly broadened. Contemporaneously, a pair of shoulders at high- and low-frequency appeared in the spectrum. These effects became more pronounced at both low temperature (see the spectrum at 200 K, in Figure 1a) and larger alcohol concentration (Figure 1b).

Figure 1b also shows that a significant broadening of the ν^{ax}_{MH} band occurred by increasing the alcohol concentration. These frequency shifts, independently of the nature of the added acid, increased steadily down the iron triad. For example, in the presence of MFE at 200 K, the $\Delta\nu^{eq}_{MH}$ values were -6 and $-12\ cm^{-1}$ for **1** and **3**, respectively, whereas $\Delta\nu^{ax}_{MH}$ amounted $+8$ and $+20\ cm^{-1}$. In agreement with an effective dependence on the nature of the metal, the frequency shifts exhibited by the ruthenium complex **2** showed intermediate values.

High-frequency shifts of ν_{MH} bands have been previously associated with the formation of M···HX hydrogen-bonding interactions where the metal acts as a proton acceptor from the proton donor HX.[1f] The behaviour of the ν_{MH} bands in

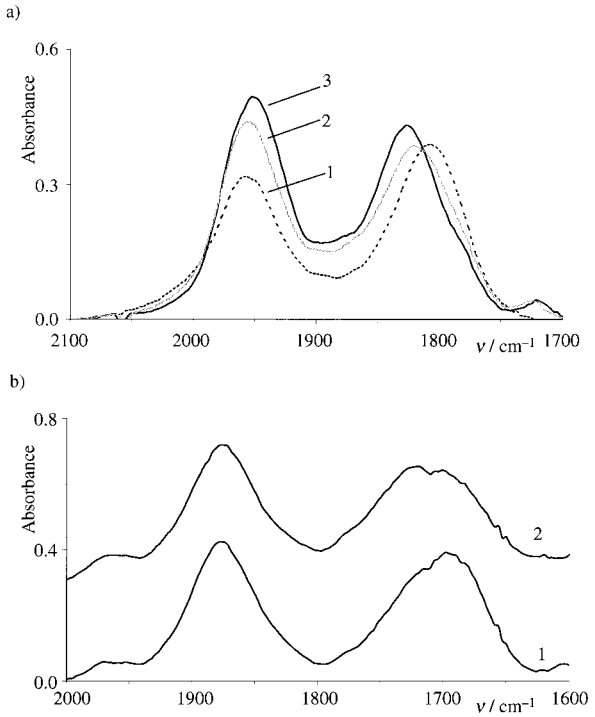

Figure 1. a) IR spectra in the range ν_{MH} of $[OsH_2(PP_3)]$ (**3**) ($c = 0.02$ M, CH_2Cl_2): without proton donor at 200 K (1); in the presence of MFE (1:10) at 200 K (2); in the presence of MFE (1:10) at 240 K (3). b) IR spectra in the range ν_{MH} of $[RuH_2(PP_3)]$ (**2**) ($c = 0.02$ M, CH_2Cl_2): without proton donor at 200 K (1): in the presence of MFE (1:2) at 200 K (2).

the presence of alcohols clearly demonstrates that either hydride ligand in **1**–**3**, and not the metal atom, is the nucleophilic site accepting the proton from the acid. Intuitively, one might suggest that the alcohol interacts with the more electron-rich $M-H^{ax}$ ligand. In this case, however, simple spectral criteria[1f] would have predicted a low-frequency shift for ν^{ax}_{MH} and an opposite high-frequency shift for ν^{eq}_{MH}. Since a more complicated change in the IR spectra was observed, we suggest that both hydride ligands participate in the DHB process as shown in Equation (1). Indeed, such non-selectivity of the proton attack would lead to an overlay of both low- and high-frequency effects giving the spectral complications observed.

$$[MH_2(PP_3)] + HOR \rightleftharpoons a[(PP_3)M(H^{eq})H^{ax}\cdots HOR)] + b[(PP_3)M(H^{ax})H^{eq}\cdots HOR)] \quad (1)$$

The results of a theoretical analysis for the reaction with MeOH are in good agreement with the hypothesis that both hydride ligands are involved in the process as the calculated DHB energies for the two hydridic sites, H^{ax} and H^{eq}, are very similar to each other despite their different electronic charges (see below). As an anticipation of the theoretical results obtained in this work, the theory predicts that H^{ax} exhibits a higher "hydridicity"[7b, c] than H^{eq} and, consequently an energetically favoured DHB to MH^{ax}, only for strong acids. Therefore, it is reasonable to expect that for weak acids, like the alcohols used in this study, H^{ax} will exhibit a higher "hydridicity"[7b,c] and will be only slightly more reactive than H^{eq} making *a* in Equation (1) only slightly greater than *b*.

Unfortunately, with TFE and other stronger acids such as HFIP and PFTB we observed a partial proton transfer that was accompanied by the appearance of new high-frequency bands. The appearance of these bands, assigned to the M–H^{eq} stretching of the nonclassical dihydrogen complexes **4**–**6**, ν_{MH}^{eq}, complicated further the spectra in the ν_{MH}^{ax} region (see, for example, Figure 2).

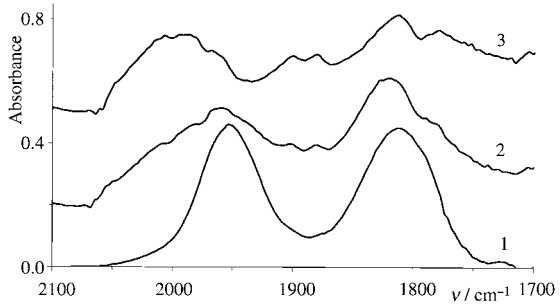

Figure 2. IR spectra in the range ν_{MH} of $[OsH_2(PP_3)]$ (**3**) ($c = 0.02$ M, CH_2Cl_2): without proton donor at 200 K (1); in the presence of TFE (1:5) at 200 K (2); at 260 K (3).

In more coordinating solvent than CH_2Cl_2, for example THF (Figure 3), a DHB process without proton transfer was observed for systems **1**–**3**/TFE. In this case the IR spectra were similar to those observed for the systems **1**–**3**/MFE in CH_2Cl_2 and the spectral changes were even more pronounced (see below).

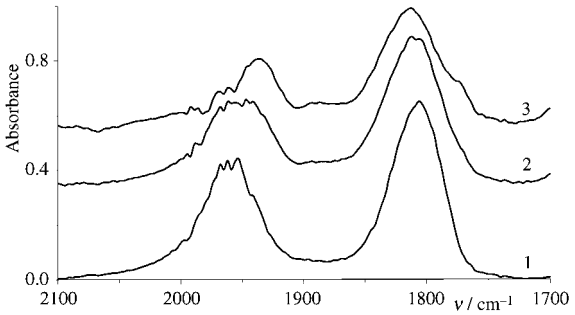

Figure 3. IR spectra in the range ν_{MH} of $[OsH_2(PP_3)]$ (**3**) ($c = 0.02$ M, THF) at 200 K: without proton donor (1); in the presence of TFE (1:10) (2); in the presence of TFE (1:20) (3).

^{1}H NMR studies: According to previous $^{31}P\{^1H\}$ and ^{1}H NMR studies,[4a–e] one can safely conclude that complexes **1**–**3** are stereochemically non-rigid in solution where the two hydride sites exhibit a temperature-dependent scrambling process. The slow exchange regime for the osmium complex was attained at 270 K, while the exchange process was frozen out at 210 and 190 K for the ruthenium and iron complexes, respectively. From an analysis of the coupling patterns of the hydrogen resonances at low temperature, the axial and equatorial hydride ligands were unequivocally assigned.[4a–e]

Previous studies have shown that the formation of hydrogen bonding may be put in evidence by a downfield shift of the OH proton signals in ^{1}H NMR spectra recorded in the same experimental conditions of the IR spectra.[1h, 2e] Therefore, we decided to examine the proton transfer process involving the dihydrides **1**–**3** by NMR spectroscopy. In view of the attainment of hydride discrimination already at 270 K, the osmium complex **3** was used for studying the DHB process by variable temperature ^{1}H NMR spectroscopy.

The proton–hydride interactions of **3** ($c = 0.03$ M) with TFE were investigated in CD_2Cl_2 between 200 and 240 K when the H/H exchange was totally frozen. At 200 K, the chemical shifts of the two hydride resonances in **3** were observed at −6.42 (H^{ax}) and −11.68 ppm (H^{eq}) in very good agreement with the literature data.[4e] The addition of a four-fold excess of TFE led to an up-field shift of the first resonance (−6.80 ppm, $\Delta\delta = -0.38$), which is typical of the H–H bond formation. The position of the second line, due to H^{eq}, (−11.65 ppm) remained practically unchanged. A similar phenomenon has been previously reported by Berke et al[7a] for the system $[H_2Re(CO)(NO)(PMe_3)]$/PFTB and interpreted in terms of preferred hydrogen bonding to the stronger-polarized hydrogen atom, located *trans* to the NO ligand. Likewise, our data demonstrate that the H^{ax} ligand, located *trans* to the bridgehead P atom, possesses a higher hydridicity[7b,c] than H^{eq} and a greater preference than the latter to interact with alcohols forming H–H bonds. The low-temperature ^{1}H NMR spectrum of the system **3**/TFE (1:4 ratio) also showed a new resonance at −7.01 ppm assigned to the molecular hydrogen ligand in the η^2-H_2 complex **6**.[4e] The occurrence of a partial proton transfer is in line with the IR data illustrated above and substantiates the greater proton-acceptor ability of **3** as compared to Berke's complex $[H_2Re(CO)(NO)(PR_3)_2]$.[7a]

In line with the previous measurements,[4e] ^{1}H NMR longitudinal-relaxation T_1 experiments on the dihydride **3**, showed that the T_1 values of both hydride ligands go through a minimum at 200–210 K with $T_{1\,min}$ values of 0.203 and 0.213 s for H^{ax} and H^{eq}, respectively. Under the same experimental conditions, variable-temperature T_1 measurements of both signals in the system **3**/TFE gave surprisingly smaller values for both $T_1(H^{ax})$ (0.120 s) and $T_1(H^{eq})$ (0.160 s) at 200 K. The shortening shown by $T_1(H^{eq})$ in the slow-motion regime is difficult to explain. A plausible hypothesis is that it may be caused by the occurrence of an efficient dipole–dipole interaction between H^{eq} and the alcohol molecule coordinated to H^{ax}. In the case of H^{ax}, the experimentally measured T_1 shortening correlates well with the up-field shift of the H^{ax} resonance caused by the formation of the H···H bonding. Moreover, the H–H distance, calculated as 1.96 Å on the basis of a standard approach,[1e,f, 2e, 7a] is actually shorter than the sum of the van der Waals radii of H (2.4 Å) and lies within the 1.7–2.2 Å interval which is typical for DHB interactions.[1f, g]

Theoretical studies: The geometrical and electronic structures of the model dihydride $[RuH_2\{P(CH_2CH_2PH_2)_3\}]$ (**7**), which is a simplified replica of **2**,[8] and its DHB complexes of the general formulas $[\{P(CH_2CH_2PH_2)_3\}RuH_2\cdots HOR]$ [ROH = CH_3OH (**8**), CF_3OH (**9**)] were calculated with the RHF/LanL2DZ method.[9, 10] The geometry and the Mulliken charges of **7** are presented in Figure 4.

Since the Mulliken population analysis is very sensitive to the basis set, the choice of a small basis set may lead to overestimation of the absolute values of atomic charges.[11, 12]

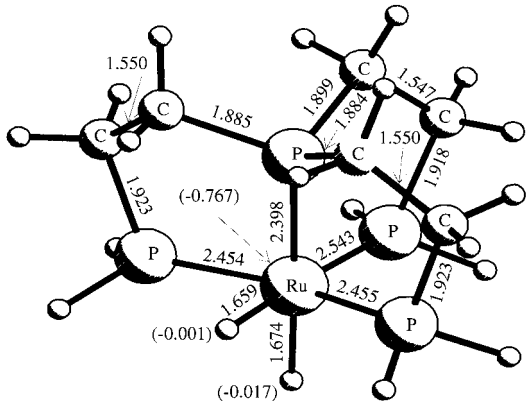

7

Figure 4. Geometry parameters for the calculated structure **7**. The bond lengths and angles are given in Å and degrees, respectively. Mulliken charges on atoms are given in parentheses.

Nonetheless, this approach is fully adequate for the description of relative tendencies.[13] According to the present theoretical analysis, the metal atom in **7** bears a large negative charge. This finding is in agreement with previous ab initio calculations on $[MH_2(L)(PP_3)]^+$ complexes (M = Fe, Ru; L = H_2, C_2H_4) and may be due to the lone pair donation from the P_4-donor set to the metal.[4f] The calculated IR frequencies ($\nu^{eq}_{MH} = 1840$ and $\nu^{ax}_{MH} = 1746$ cm^{-1}) are reported in Table 3 and are in excellent agreement with the experimental data (Table 1). In keeping with the experimental assignments discussed above, the calculated ν^{eq}_{MH} values are considerably larger than ν^{ax}_{MH}.

The optimised geometries and Mulliken charges for the DHB compounds **8** and **9** are shown in Figures 5 and 6, while Table 3 reports the energy characteristics, the harmonic vibrations of the Ru–H bonds and the H–H overlap populations for the model complexes.

A perusal of Table 3 shows that the Ru–H bond involved in the DHB interaction is significantly stretched. This feature

Table 3. Total energies (E_{total}/hartrees), relative energies (ΔE/kcal mol^{-1}) and harmonic vibrational frequency (ν/cm^{-1}) for RuH^{ax} and RuH^{eq} bonds calculated by RHF/LanL2DZ method and Mulliken population bond analysis (p_{RuH} and $p_{H\cdots H}$).

Structure	E_{total}	ΔE	ν^{ax}_{RuH}	ν^{eq}_{RuH}	p^{ax}_{RuH}	p^{eq}_{RuH}	$p_{H\cdots H}$
7	–357.004267	–	1746	1840	0.343	0.358	
8^{ax}	–472.035757	0	1713	1839	0.322	0.361	0.022
8^{eq}	–472.035714	0.02	1748	1823	0.343	0.317	0.034
9^{ax}	–768.628117	0	1723	1861	0.265	0.360	0.101
9^{eq}	–768.622669	3.42	1821	1739	0.339	0.262	0.120

together with the practically linear arrangement of the OH–H moiety and the bending of the MH–H bond are very similar to those found for a variety of DHB complexes involving transition-metal monohydrides.[1f, 2]

Upon OH proton attack at the axial hydride, the Ru–H^{ax} bond elongation is accompanied by a shortening of the Ru–H^{eq} bond. Noticeably, the extent of these two synchronous changes ($\Delta(r)$), increase with the acidic strength of the added alcohol ($\Delta(r) = +0.016$ (RuH^{ax}) and -0.002 (RuH^{eq}) for CH_3OH (Figure 5a); $+0.031$ (RuH^{ax}) and -0.009 (RuH^{eq}) for CF_3OH (Figure 6a). A similar trend was calculated when the attack was carried out at the H^{eq} atom: $\Delta(r) = +0.010$ (RuH^{eq}) and -0.004 (RuH^{ax}) for CH_3OH (Figure 5b) and $+0.032$ (RuH^{eq}) and -0.014 (RuH^{ax}) for CF_3OH, respectively (Figure 6b). It is also worth noticing that the values of the H–H overlap population (Table 3) featuring the DHB interaction increase with the alcohol acidity from 0.002–0.034 (CH_3OH) to 0.101–0.120 (CF_3OH).

The complexation energies, computed as the differences between the total energies of the complexes and the sum of the total energies of the isolated molecules, have been found to increase with the proton-donating ability of the alcohol from 9.70 to 20.77 kcal mol^{-1} for OH–H^{ax} and from 9.68 to 17.35 kcal mol^{-1} for OH–H^{eq} (Table 3). A relevant feature of this study is that any energetic preference for the DHB interaction with H^{ax} is practically negligible for weaker proton donors ($\Delta\Delta E = 0.02$ kcal mol^{-1}), yet it becomes effective as

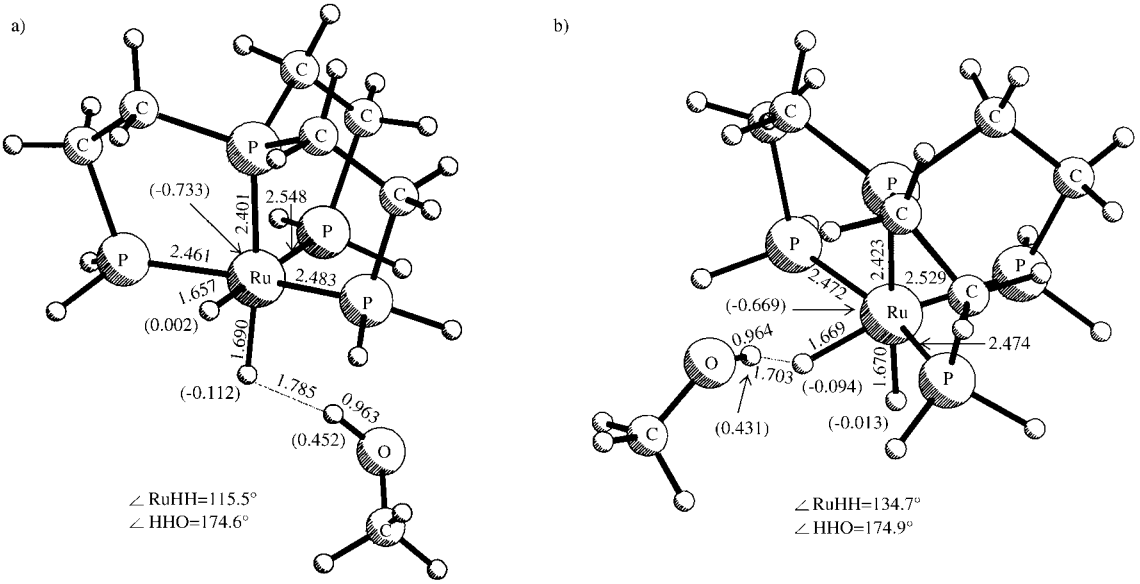

Figure 5. Geometry parameters of calculated isomers **8**^{ax} and **8**^{eq}. The bond lengths and angles are given in Å and degrees, respectively.

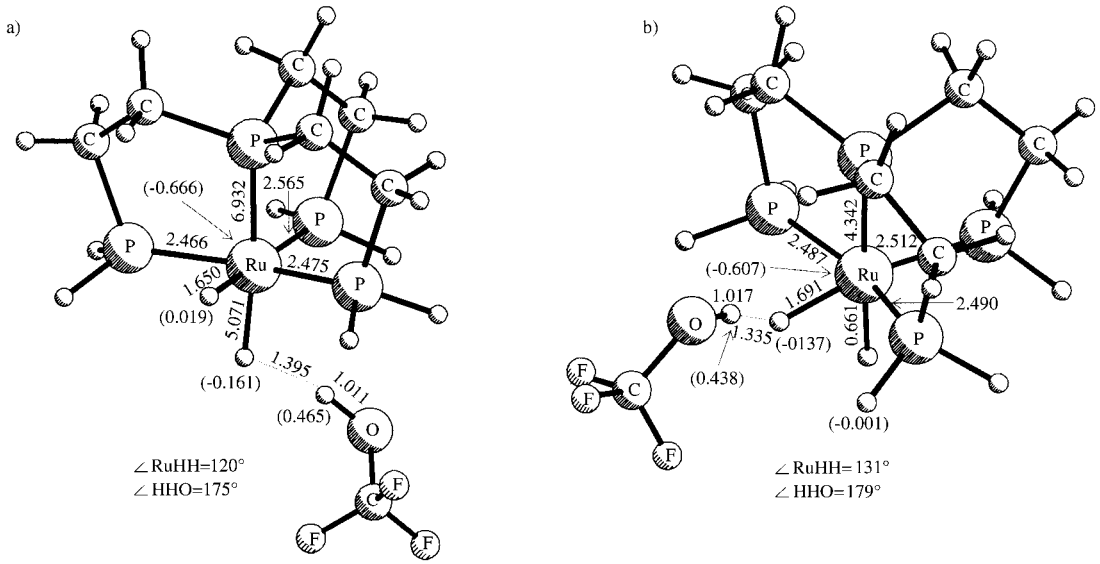

Figure 6. Geometry parameters of calculated isomers $\mathbf{9}^{ax}$ and $\mathbf{9}^{eq}$. The bond lengths and angles are given in Å and degrees, respectively.

soon as stronger proton donors are considered ($\Delta\Delta E =$ 3.42 kcal mol^{-1}). As a general effect, the occurrence of a DHB interaction increases the negative charge of the H atoms involved in this bonding and slightly decreases the electron density of the non-bonded hydrogen atoms. Significant polarization of the M–H bonds in complexes with DHB has been also reported for other systems.[13]

Notably, the calculated IR changes of ν_{MH} modes match the spectral criteria established by experimental studies.[1f] Therefore, the bands of the coordinated and free M–H bonds shift down and up, respectively (see for example $\mathbf{8}^{ax}$, $\mathbf{8}^{eq}$ and $\mathbf{9}^{ax}$ in comparison with **7** in Table 3). However, the calculated negative shift of the ν_{MH}^{eq} band, following the attack of CH_3OH at H^{ax}, is, although very small (-1 cm^{-1}, $\mathbf{8}^{ax}$), unexpected, while the shift experienced by the band assigned to the bonded H^{eq} (-7 cm^{-1}, $\mathbf{8}^{eq}$) agrees well with the experimental shift observed for **2** in the presence of MFE. The magnitude of these shifts, particularly those involving the bonding interaction OH$\cdots$H^{eq}, increases as soon as the alcoholic proton becomes more acidic and, for the DHB complex involving CF_3OH ($\mathbf{9}^{eq}$), such trend leads to the mutual exchange of the two stretching modes: ν_{MH}^{ax} (1821 cm^{-1}) $> \nu_{MH}^{eq}$ (1739 cm^{-1}) (Table 3 and Figure 6b).

In conclusion, the theoretical results confirm the experimental assignment of the two ν_{MH} bands and support the experimental finding indicating that a DHB interaction takes place involving both hydride ligands. Noticeably, the calculations predict that an energetically favoured interaction involving the axial hydride site, MH$^{ax}\cdots$HO swells up with more acidic alcohols. Other remarkable outcomes of the theoretical analysis are: i) a good agreement with the main structural features of the DHB complexes, ii) a change of the charge redistribution, which follows the intermolecular complexation of the acid substrate with the two different M–H bonds and iii) a good correlation between the coordination site and the energy of the DHB interaction with the proton donor strength.

The strength of the MH$\cdots$HX bond and the proton-accepting ability of the hydride ligand as a function of the metal atom: The enthalpies of dihydrogen bond formation, $-\Delta H^\circ$, between the metal dihydrides and the alcohols under investigation were obtained by two independent methods based on either the analysis of the IR spectral data, that is using the empirical correlation shown in Equation (2), originally established for classical hydrogen bonds[14] and later extended to DHB complexes,[1d, g, e, 3a] or the van't Hoff method. This procedure was applied to the systems **1**/TFE and **3**/TFE:

$$-\Delta H^\circ = 18\Delta\nu/(\Delta\nu + 720) \qquad (2)$$

The changes in the $\nu_{OH(free)}$ intensities were measured at different temperatures in order to obtain reliable values of the equilibrium constant K_f of Equation (1). The K_f values were obtained measuring the optical densities of $\nu_{OH(free)}$ at different temperatures between 200 and 270 K. The corresponding van't Hoff plots ($\ln K_f$ versus $1/T$, see Figure 7) allowed us to calculate the thermodynamic parameters associated with DHB formation.

The enthalpy values obtained with the two methods were in excellent agreement as the same $-\Delta H^\circ$ value of

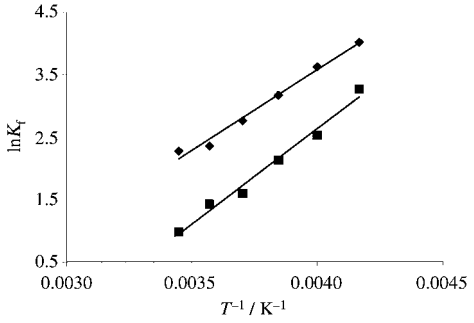

Figure 7. Van't Hoff plot of the hydrogen bonding of **1** (◆) and **3** (■) ($c =$ 0.06 M) with TFE ($c = 0.015$ M) at 230–290 K.

6.8 kcal mol^{-1} was calculated for the osmium system **3**/TFE, in fact, while for the iron analogue, **1**/TFE, $-\Delta H^{\circ}$ values of 4.5 and 5.1 kcal mol^{-1} were determined from Equation (2) and the van't Hoff plot, respectively.

Table 4 shows that all the dihydrogen bonds involving the dihydrides **1**–**3** are featured by medium strength ($-\Delta H^{\circ}$ = 3.3–6.8 kcal mol^{-1}) and become more stable as the proton-donor ability of the alcohol increases, following the order MeOH < MFE < TFE < HFIP. Finally, it is worth mentioning that also the entropy values, $-\Delta S^{\circ}$, calculated by the van't Hoff method as 19.2 and 13.4 e.u. for **3**/TFE and **1**/TFE, respectively, are within the range reported for other dihydrogen bonds (5–22 e.u.).[1f]

The Iogansen basicity factor, E_j, defined by Equation (3),[14, 15] may be used to compare the proton-accepting ability of the three dihydrides **1**–**3**. The E_j values were obtained from the experimental values of $-\Delta H^{\circ} = -\Delta H_{ij}$, the known proton-donor ability of the alcohols, P_i,[14a] and the enthalpy, $-\Delta H_{11}$, of the standard hydrogen-bonded adduct related to the system phenol/Et_2O (4.6 kcal mol^{-1}) in CH_2Cl_2[14a, 15]:

$$E_j = \Delta H_{ij}/(\Delta H_{11} P_i) \quad (3)$$

Table 4. Enthalpy values ($-\Delta H^{\circ}$/kcal mol^{-1}) of H···H bonds and basicity factors (E_j) for the hydride ligands.

	XH	P_i	$-\Delta H^{\circ}$	E_j[a]
	MeOH	0.63	3.3	1.13
$[FeH_2(PP_3)]$ (**1**)	MFE	0.74	3.8	1.12
	TFE	0.89	4.5[b]	1.10
	*i*PrOH	0.58	3.6	1.35
$[RuH_2(PP_3)]$ (**2**)	TFE	0.89	5.4	1.32
	HFIP	1.05	6.4	1.33
	MeOH	0.63	4.8	1.66
$[OsH_2(PP_3)]$ (**3**)	MFE	0.74	5.8	1.70
	TFE	0.89	6.7[c]	1.64

[a] $E_j = 1.12 \pm 0.02$ (**1**), 1.33 ± 0.02 (**2**), 1.67 ± 0.03 (**3**). [b] $-\Delta H^{\circ}$ = 5.1 kcal mol^{-1}, $-\Delta S^{\circ}$ = 13.4 e.u. [c] $-\Delta H^{\circ}$ = 6.8 kcal mol^{-1}, $-\Delta S^{\circ}$ = 19.2 e.u. by the van't Hoff method.

The E_j values reported in Table 4 are actually independent of the proton-donor strength, P_i, and show that the proton-accepting ability of the hydride ligands steadily increases from iron to osmium: E_j {H(Fe)} 1.09 < E_j {H(Ru)} 1.32 < E_j {H(Os)} 1.67. The same group tendency (Fe < Ru < Os) was previously established for XH···M bonding.[1b] A perusal of Table 4 also reveals that **2** and **3** are stronger bases than DMSO ($E_j = 1.27$) and that **3** exhibits the same E_j value of pyridine ($E_j = 1.67$).[14a] A comparison of the E_j factor of **2** with those determined for other ruthenium hydrides suggests that **2** is a slightly weaker base than $[RuH_2(CO)(triphos)]$ (E_j = 1.39), and $[RuH_2(dppm)_2]$ ($E_j = 1.40$),[1i] yet it is significantly stronger than $[CpRuH(CO)(PCy_3)]$ ($E_j = 1.00$).[3d] Finally, it is worth noticing that the basicity factor determined for **3** is the highest reported so far for transition-metal hydrides.[1i]

Proton transfer through H···H bonding: In line with the high values of their E_j factors, the dihydrides **1**–**3** were readily protonated, even by weak acids such as fluorinated alcohols to give the hydride–dihydrogen complexes $[MH(\eta^2\text{-}H_2)(PP_3)]^+$ (**4**–**6**) [Eq. (4)].[1f] As discussed above, while MFE formed DHB adducts only in the presence of a large excess of the proton donor, TFE gave rise to proton transfer (as specifically confirmed by ^{1}H NMR data for the system **3**/TFE, see below) also using an excess of the alcohol.

The interactions between the hydrides **1**–**3** and the strong acid HBF_4 in CH_2Cl_2 were preliminarily studied in order to

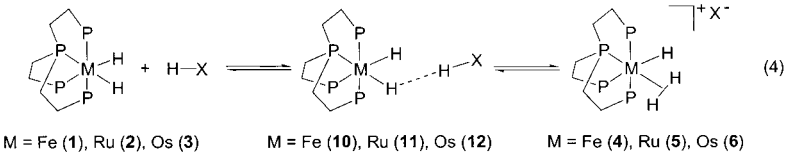

M = Fe (**1**), Ru (**2**), Os (**3**) M = Fe (**10**), Ru (**11**), Os (**12**) M = Fe (**4**), Ru (**5**), Os (**6**) (4)

establish which spectral changes in the ν_{MH} region accompany the complete proton transfer leading to the cationic dihydrogen complexes **4**–**6**. These spectral modifications are caused by the replacement of the initial hydride bands with weaker and broad high-frequency shifted bands, ν_{MH}^{eq}, due to the terminal hydride ligand in **4**–**6**. The latter IR absorptions [1912 cm^{-1} for Ru and 2012 cm^{-1} for Os] coincide with those measured in CH_2Cl_2 for the protonation of the dihydrides **1**–**3** with HBF_4 as well as those exhibited by CH_2Cl_2 solutions of the isolated salts $[MH_2(\eta^2\text{-}H_2)(PP_3)]BPh_4$. A similar upshot was found in the solid-state IR spectra showing bands at 1930 (**5**) and 2050 cm^{-1} (**6**).[4] Unfortunately, the stretching vibrations of the H–H ligand, $\nu_{(H_2)}$, and the $\nu_{(M\text{–}H_2)}$ bands were not observed in either CH_2Cl_2 solution or solid state spectra, as they are too weak and probably masked by more intense $\nu_{C\text{–}H}$ or $\nu_{C\text{–}C}$ absorptions.[4]

The proton transfer from reaction with TFE was studied in CH_2Cl_2 by varying the ratio between the metal hydride and TFE from 1:3 to 1:10. Under these experimental conditions, the new high-frequency band appeared as a combination of three bands assigned to ν_{MH}^{eq} of **4**–**6**, ν_{MH}^{eq} of **10**–**12** and ν_{MH}^{eq} of **1**–**3** (see Figure 2). Either increasing the alcohol concentration or decreasing the temperature shifted to the right the equilibrium shown in Equation (4) demonstrating the complete reversibility of the system.

The hydrogen-transfer process transforming **1**–**3** into **4**–**6** was completely reversible in CH_2Cl_2 within a broad interval of concentrations and temperatures (200–290 K) only for the osmium hydride **3.** The dihydrides **1** and **2** underwent a slow H^{ax}/Cl exchange at above 250 K in fact (this was shown by the decreasing of the ν_{MH}^{ax} bands with time). A complete reversibility for **1** and **2** was demonstrated in "inert" solvents such as THF, however.

The less polar ($\varepsilon = 7.32$), yet better coordinating solvent, THF competed with the metal hydride in forming hydrogen bonds[3a, 7a] diminishing DHB formation constants and strength, and therefore, inhibited the proton transfer process. So, the IR spectra of a THF solution of **3** (the most basic hydride) showed the occurrence of DHB only in the presence of a large excess of TFE (Figure 3). Thus, at variance with

CH_2Cl_2 ($\varepsilon = 8.9$), when **1-3** were dissolved in THF (Figure 8) a stronger alcohol (HFIP) was necessary to highlight the occurrence of proton transfer.

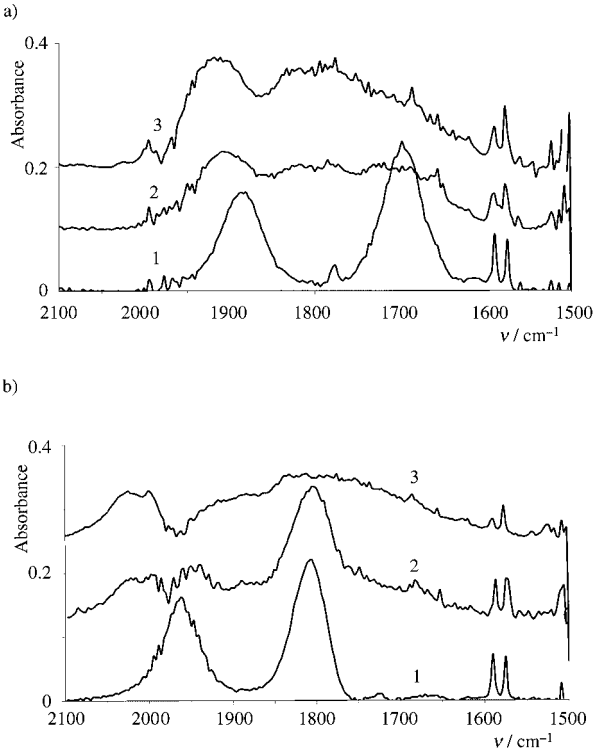

Figure 8. a) IR spectra in the range ν_{MH} of $[RuH_2(PP_3)]$ (**2**) at 200 K in THF: without proton donor (1); in the presence of HFIP (1:6) (2), in the presence of HFIP (1:10) (3). b) IR spectra in the range ν_{MH} of $[OsH_2(PP_3)]$ (**3**) at 200 K in THF: without proton donor (1); in the presence of HFIP (1:5) (2); in the presence of HFIP (1:10) (3).

In this case, the effects of **1**–**3**/HFIP ratio and temperature were similar to those observed in CH_2Cl_2 for interaction with TFE (Figure 2). For example, the high-frequency ν_{MH}^{eq} band of **2** shifted from 1874 to 1905 and 1920 cm^{-1} when an excess of HFIP was used (Figure 8a). The osmium hydride, **3** showed a similar behaviour (Figure 8b). At low temperature and high alcohol concentration, an extremely broad "continuous" absorption in the range 1850–1650 cm^{-1} was unexpectedly observed (see Figure 8 and trace 3 in Figure 2). "Continuous" IR absorptions have been previously reported for either symmetrical ionic hydrogen bonds or hydrogen-bonded quasi-ionic structures and have been explained in terms of important mixing of proton vibrations with different normal modes of the organic base.[16] In the case at hand, the interpretation of this spectral perturbation denies any simple interpretation and requires deeper theoretical and experimental studies to be assessed without ambiguity.

One of the major objectives of this study, that is the quantitative characterisation of the proton-transfer reactions as a function of the hydride-supporting metal, could not be completely accomplished. Indeed, the energy values associated with the single stages of the process shown in Equation (4) could be determined only for the osmium complex **3**. Only the complex $[OsH(\eta^2\text{-}H_2)(PP_3)](OCH_2CF_3)$ was stable between 200 and 290 K in CH_2Cl_2 in fact, which allowed us to observe simultaneously the three species involved in the equilibrium. The enthalpy relative to the formation of the hydrogen-bonded adduct **12** was determined as 6.8 kcal mol^{-1} in the case of TFE by IR methods (see above). The energy associated with the transformation of **12** into **6** was obtained by both IR and ^1H NMR data for **3**/TFE in CD_2Cl_2. The equilibrium constants related to the latter transformation, $K_{\mathbf{12}\rightarrow\mathbf{6}}$, were determined in the ranges 190–290 K (IR) and 200–240 K (NMR) (Table 5).

Table 5. Values of the equilibrium constants, $K_{\mathbf{12}\rightarrow\mathbf{6}}$, obtained from variable temperature IR and NMR spectra for **3** in the presence of ten-fold TFE excess.[a]

T [K]	$K_{\mathbf{12}\rightarrow\mathbf{6}}$	
	A (from IR data)	**B** (from NMR data)
290	1.41	
270	1.95	
250	3.79	
240		3.72
230		5.24
220	6.14	7.71
210	7.89	8.42
200		10.46
190	14.18	

[a] **A**: $-\Delta H^\circ = 2.5$ kcal mol^{-1}, $-\Delta S^\circ = 7.7$ e.u. **B**: $-\Delta H^\circ = 2.4$ kcal mol^{-1}, $-\Delta S^\circ = 7.2$ e.u.

Since the free dihydride **3** was not observed in the presence of a large excess of TFE (ca. 10 equivalents), the equilibrium constant, $K_{\mathbf{12}\rightarrow\mathbf{6}}$, was calculated from the optical density of the IR high-frequency band, ν_{MH}^{eq}, of **6** (2012 cm^{-1}) and from the integration of the ^1H NMR hydride resonance of **6** (−7.0 ppm) and **12** (−6.7 ppm). Remarkably, the enthalpy value $-\Delta H^\circ_{\mathbf{12}\rightarrow\mathbf{6}}$ determined from the $K_{\mathbf{12}\rightarrow\mathbf{6}}$ constants, was practically independent of the method used (2.5 vs 2.4 kcal mol^{-1}, Table 5). Finally, the total energy gain for the process in Equation (4) was calculated to be about 9.6–9.4 kcal mol^{-1}, with the DHB step contributing to the major part of the total energy gain.

Incorporation of all these data allowed us to trace the energy profile of the proton-transfer reaction transforming **3** into **6** via the H-bonded intermediate **12** (Scheme 2). In such a plot, the abscissa is the reaction coordinate in which the proton-hydride distance, $r_{(H\text{–}H)}$, was calculated for **12** by ^1H NMR relaxation data, $r = 1.96$ Å and determined before for **6** with $r = 0.95$ Å.[4e] While the formation of the hydrogen-bonded adduct (**3** → **12**) is a diffusion-controlled process with no energy barrier,[17] the activation barrier for the second step (**12** → **6**) could not be determined. Therefore, the energy level of the transition state for the proton transfer in Scheme 2 was semi-quantitatively estimated using the procedure previously adopted by us.[18] Noticeably, this method gave an energy barrier in agreement with recently reported theoretical[13] and experimental data.[3d, 19]

The potential energy curve illustrated in Scheme 2 shows two minima: one corresponding to the formation of the hydrogen-bonded species **12**, the other, at lower energy, corresponding to the dihydrogen complex **6.**

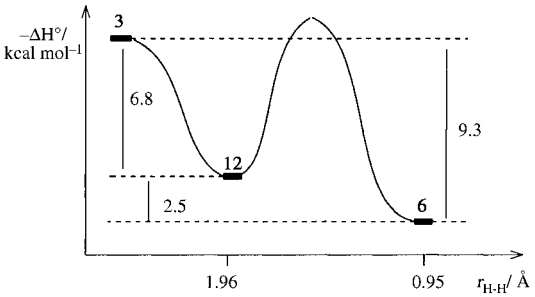

Scheme 2. Energy profile for the conversion of $[OsH_2(PP_3)]$ (**3**) into $[Os(H)(H_2)(PP_3)]^+$ (**6**) via $[(PP_3)OsH_2\cdots HOR]$ (**12**) [Eq. (4)].

Conclusion

We have studied the protonation reactions which transform iron, ruthenium and osmium classical dihydrides into non-classical hydrido-dihydrogen complexes in the temperature range from 200 to 290 K discovering that dihydrogen-bonded adducts M-H$\cdots$HOR (DHB) are intermediate species along the proton-transfer process. An analysis of the spectral changes associated with this process, using a variety of alcohols with different proton donor strength, showed that both hydride ligands of the $[MH_2(PP_3)]$ precursors are involved in the proton-transfer process when weak proton donors are employed. In contrast, a preference for the formation of a DHB species involving selectively the H^{ax} ligand was established for more acidic alcohols. A theoretical study corroborated the experimental studies. The thermodynamic properties of the DHB intermediates imply that the proton accepting ability of the hydride ligands of the $[MH_2(PP_3)]$ increases in going down the iron triad (Fe−H < Ru−H < Os−H). The energy diagram of the proton transfer reaction was determined for the $[OsH_2(PP_3)]$/TFE system. A double-minima energy profile was established in which a significant contribution to the total energy gain representing the driving force to the formation of the η^2-H_2 species is assigned to the DHB energy.

Experimental Section

The dihydrides $[MH_2(PP_3)]$ (**1**–**3**) and the molecular hydrogen complexes $[M(H)(H_2)(PP_3)]Y$ ($Y = SO_3CF_3^-$, BF_4^-) were prepared as previously described.[4] Tetrahydrofuran (THF) was freshly distilled over $LiAlH_4$ and CH_2Cl_2 was purified by distillation over CaH_2 before use. The anhydrous solvents were thoroughly degassed prior to use. All samples were prepared under dry argon atmosphere using standard Schlenk techniques.

IR measurements were carried out on a "Specord M82" spectrometer using 0.1 cm CaF_2 cells. Low-temperature IR measurements were carried out in CH_2Cl_2 and THF using a Carl Zeiss Jena cryostat in the temperature range 190 to 300 K using a stream of liquid nitrogen. The accuracy of the experimental temperature was ±0.5 K. The cell width was 0.04–0.12 cm. The reagents were mixed at low temperatures to prevent the formation of the η^2-H_2 complexes and the cold solutions were transferred into the cryostat pre-cooled to the required temperature. In the IR studies, the concentration of **1**–**3** in either THF or CH_2Cl_2 solutions was between 10^{-1} and 10^{-3} M. These concentrations refer to room temperature conditions and were not corrected for the working temperature of 200 K at which most of the IR studies were performed.

The Raman spectra were obtained by excitation with the green 514.5 nm line of an Argon laser (Coherent, Innova 90). The back-scattered light was collected and focused into a double monochromator (Jobin-Yvon HG2S 2000) equipped with a cooled photomultiplier (RCA C31034A). The spectral frequencies were calibrated with CCl_4 as a standard.

The ^{1}H NMR spectra were recorded on Bruker WP-200 and AMX 400 spectrometers and were calibrated with respect to tetramethylsilane as external reference. The conventional inversion-recovery method (180-τ-90) was used to determine the variable-temperature longitudinal-relaxation time T_1. The calculation of the relaxation times was made using the nonlinear three-parameter fitting routine of the spectrometers. In each experiment, the waiting period was five times larger than the expected relaxation time and 16–20 variable delays were employed. The duration of the pulses were controlled at every temperature. The errors in T_1 determinations were lower than 5% (this was checked with different samples).

All the stationary point optimisation calculations in this work were performed by standard restricted Hartree-Fock method[9] with pseudopotential quasi-relativistic basis set LanL2DZ using the Gaussian 98 packages of ab initio programs.[10] Optimisation of molecular geometry at stationary points was carried out using the "tight" convergence criterion in order to obtain accurate harmonic vibrational frequencies. Force constants were calculated by analytical method. All the results obtained relate to the gas phase. No counterpoise corrections were made for the basis set superposition error (BSSE)[20] in calculations concerned energy hydrogen bonding because the inclusion of BSSE often may enormously decrease the thermodynamic stability and binding energy in multimolecular assemblies.[21–25]

Acknowledgements

Authors thank Dr. Alessandro Feis (University of Florence) for his kind assistance with the Raman spectra measurements. INTAS (00-00179), Russian Foundation for Basic Research (02-03-32194, 02-03-06381, 02-03-06380), EC (RTN HPRN-CT-2002-00176) and CNR/RAS bilateral agreement (2002/2003) are also acknowledged for promoting this scientific activity and for financial support.

[1] a) R. H. Crabtree, P. E. M. Siegbahn, O. Eisenstein, A. L. Rheingold, T. F. Koetzle, *Acc. Chem. Res.* **1996**, *29*, 348–354; b) E. S. Shubina, N. V. Belkova, L. M. Epstein, *J. Organomet. Chem.* **1997**, *536–537*, 17–29; c) J. C. M. Rivas, L. Brammer, *Coord. Chem. Rev.* **1999**, *183*, 43–80; d) E. S. Shubina, N. V. Belkova, E. V. Bakhmutova, L. N. Saitkulova, A. V. Ionidis, L. M. Epstein, *Izv. Akad. Nauk Ser. Khim.* **1998**, 846–851 (E. S. Shubina, N. V. Belkova, E. V. Bakhmutova, L. N. Saitkulova, A. V. Ionidis, L. M. Epstein, *Russ. Chem. Bull.* **1998**, *47*, 817–822); e) R. H. Morris, in *Recent Advances in Hydride Chemistry* (Eds.: M. Peruzzini, R. Poli), Elsevier, Amsterdam, NL, **2001**, Chapter 1, p. 1–38; f) N. V. Belkova, L. M. Epstein, E. S. Shubina, in *Recent Advances in Hydride Chemistry* (Eds.: M. Peruzzini, R. Poli), Elsevier, Amsterdam, NL, **2001**, Chapter 14, p. 391–418; g) E. Clot, O. Eisenstein, D.-H. Lee, R. H. Crabtree, in *Recent Advances in Hydride Chemistry* (Eds.: M. Peruzzini, R. Poli), Elsevier, Amsterdam, NL, **2001**, Chapter 3, p. 75–88; h) A. Albinati, V. I. Bakhmutov, N. V. Belkova, C. Bianchini, L. M. Epstein, I. de los Ríos, E. I. Gutsul, L. Marvelli, M. Peruzzini, R. Rossi, E. S. Shubina, E. V. Vorontsov, F. Zanobini, *Eur. J. Inorg. Chem.* **2002**, 1530–1539; i) E. S. Shubina, L. M. Epstein, *Coord. Chem. Rev.* **2002**, *231*, 165–181.

[2] a) J. A. Ayllon, C. Gervaux, S. Sabo-Etienne, B. Chaudret, *Organometallics* **1997**, *16*, 2000–2002; b) S. Gruendemann, S. Ulrich, H.-H. Limbach, N. S. Golubev, G. S. Denisov, L. M. Epstein, S. Sabo-Etienne, B. Chaudret, *Inorg. Chem.* **1999**, *38*, 2550–2551; c) L. M. Epstein, E. S. Shubina, *Ber. Bunsen-Ges. Phys. Chem.* **1998**, *102*, 359–363; d) E. S. Shubina, N. V. Belkova, E. V. Bakhmutova, E. V. Vorontsov, V. I. Bakhmutov, A. V. Ionidis, C. Bianchini, L. Marvelli, M. Peruzzini, L. M. Epstein, *Inorg. Chim. Acta* **1998**, *280*, 302–306; e) N. V. Belkova, E. S. Shubina, L. M. Epstein, S. E. Nefedov, I. L. Eremenko, *J. Organomet. Chem.* **2000**, *610*, 58–70.

[3] a) E. S. Shubina, N. V. Belkova, A. N. Krylov, E. V. Vorontsov, L. M. Epstein, D. G. Gusev, M. Niedermann, H. Berke, *J. Am. Chem. Soc.* **1996**, *118*, 1105 – 1112; b) N. V. Belkova, E. S. Shubina, A. V. Ionidis, L. M. Epstein, H. Jacobsen, A. Messmer, H. Berke, *Inorg. Chem.* **1997**, *36*, 1522 – 1525; c) E. S. Shubina, N. V. Belkova, A. V. Ionidis, N. S. Golubev, S. N. Smirnov, P. Schah-Mohammedi, L. M. Epstein, *Izv. Akad. Nauk Ser. Khim.* **1997**, 1405 – 1406 (E. S. Shubina, N. V. Belkova, A. V. Ionidis, N. S. Golubev, S. N. Smirnov, P. Schah-Mohammedi, L. M. Epstein, *Russ. Chem. Bull.* **1997**, *44*, 1349 – 1350); d) N. V. Belkova, A. V. Ionidis, L. M. Epstein, E. S. Shubina, St. Gruendemann, N. S. Golubev, H.-H. Limbach, *Eur. J. Inorg. Chem.* **2001**, 1753 – 1761; e) E. T. Papish, M. P. Magree, J. R. Norton, in *Recent Advances in Hydride Chemistry* (Eds.: M. Peruzzini, R. Poli), Elsevier, Amsterdam (The Netherlands), NL, **2001**, Chapter 2, p. 39 – 74.

[4] a) C. Bianchini, P. J. Perez, M. Peruzzini, A. Vacca, F. Zanobini, *Inorg. Chem.* **1991**, *30*, 279 – 287; b) C. Bianchini, F. Laschi, M. Peruzzini, M. F. Ottaviani, A. Vacca, P. Zanello, *Inorg. Chem.* **1990**, *29*, 3394 – 3402; c) C. Bianchini, M. Peruzzini, A Polo, A. Vacca, *Gazz. Chim. Ital.* **1991**, *121*, 543 – 549; d) C. Bianchini, A. Meli, M. Peruzzini, P. Frediani, C. Bohanna, M. A. Esteruelas, L. A. Oro, *Organometallics* **1992**, *11*, 138 – 145; e) C. Bianchini, K. Linn, D. Masi, C. Mealli, M. Peruzzini, A. Polo, A. Vacca, F. Zanobini, *Inorg. Chem.* **1993**, *32*, 2366 – 2376; f) C. Bianchini, D. Masi, M. Peruzzini, M. Casarin, C. Maccato, G. A. Rizzi, *Inorg. Chem.* **1997**, *36*, 1061 – 1069; g) V. I. Bakhmutov, C. Bianchini, F. Maseras, A. Lledos, M. Peruzzini, E. V. Vorontsov, *Chem. Eur. J.* **1999**, *5*, 3318 – 3225.

[5] a) R. B. Girling, P. Grebenic, R. N. Perutz, *Inorg. Chem.* **1986**, *25*, 31 – 36; b) B. Ma, C. L. Collins, H. F. Schaefer III, *J. Am. Chem. Soc.* **1996**, *118*, 870 – 879.

[6] C. Mealli, C. A. Ghilardi, A. Orlandini, *Coord. Chem. Rev.* **1992**, *120*, 361 – 387.

[7] a) A. Messmer, H. Jacobsen, H. Berke, *Chem. Eur. J.* **1999**, *5*, 3341 – 3349; b) S. Feracin, T. Burgi, V. I. Bakhmutov, I. L. Eremenko, E. V. Vorontsov, A. V. Vymenits, H. Berke, *Organometallics* **1994**, *13*, 4194 – 4202; c) H. Jacobsen, H. Berke, in *Recent Advances in Hydride Chemistry* (Eds.: M. Peruzzini, R. Poli), Elsevier, Amsterdam (The Netherlands), **2001**, Chapter 4, p. 89 – 116.

[8] The osmium complex **3** was not studied theoretically because the pseudopotential relativistic basis set Lanl2DZ gave poor agreement with the experimental data.

[9] B. Foresman, A. Frisch in *Exploring chemistry with electronic structure methods*, Gaussian, Inc., Pittsburg, PA, **1996**.

[10] Gaussian 98 (Revision A.7), M. J. Frisch, G. W. Trucks, H. B. Schlegel, G. E. Scuseria, M. A. Robb, J. R. Cheeseman, V. G. Zakrzewski, J. A. Montgomery, R. E. Stratmann, J. C. Burant, S. Dapprich, J. M. Millam, A. D. Daniels, K. N. Kudin, M. C. Strain, O. Farkas, J. Tomasi, V. Barone, M. Cossi, R. Cammi, B. Mennucci, C. Pomelli, C. Adamo, S. Clifford, J. Ochterski, G. A. Petersson, P. Y. Ayala, Q. Cui, K. Morokuma, D. K. Malick, A. D. Rabuck, K. Raghavachari, J. B. Foresman, J. Cioslowski, J. V. Ortiz, B. B. Stefanov, G. Liu, A. Liashenko, P. Piskorz, I. Komaromi, R. Gomperts, R. L. Martin, D. J. Fox, T. Keith, M. A. Al-Laham, C. Y. Peng, A. Nanayakkara, C. Gonzalez, M. Challacombe, P. M. W. Gill, B. G. Johnson, W. Chen, M. W. Wong, J. L. Andres, M. Head-Gordon, E. S. Replogle, J. A. Pople, Gaussian, Inc., Pittsburgh, PA, **1998**.

[11] a) J. Cioslowski, P. R. Surjan, *Theochem* **1992**, *255*, 9 – 19; b) F. Maseras, A. Lledos, E. Clot, O. Eisenstein, *Chem. Rev.* **2000**, *100*, 601 – 636.

[12] M. L. McKee, *J. Am. Chem. Soc.* **1993**, *115*, 2818 – 2825.

[13] G. Orlova, S. Scheiner, *J. Phys. Chem. A* **1998**, *102*, 4813 – 4818.

[14] a) A. V. Iogansen, *Theor. Experim. Khim.* **1971**, 302 – 320; b) A. V. Iogansen, *The Hydrogen Bond*, Moscow, Nauka, **1981**, 112 – 155; c) A. V. Iogansen, *Spectrochim. Acta A* **1999**, *55*, 1585 – 1594.

[15] The empirical Iogansen "rule of factors"[14a] demonstrating the invariability of both proton donor (P_i) and proton acceptor (E_j) properties of organic acids and bases in hydrogen bonding was obtained from a large array of spectral data. We used the following equation of "rule of factors" $(-\Delta H_{ij}) = (-\Delta H_{11}) P_i E_j$, where $(-\Delta H_{11})$ is the enthalpy of hydrogen bonding for the standard pair phenol/diethyl ether ($P_{11} = E_{11} = 1.00$).

[16] a) G. V. Yuchnevich, E. G. Tarakanova, V. D. Maiorov, N. B. Libroich, *J. Mol. Struct.* **1992**, *265*, 237 – 240; b) A. Hayd, E. G. Weidemann, G. Zundel, *J. Chem. Phys.* **1979**, *70*, 86 – 92; c) V. D. Maiorov, S. G. Sysoeva, O. N. Temkin, I. S. Kislina, *Bull. RAS Ser. Khim.* **1993**, 1577 – 1582; d) J. P. Castaneda, G. S. Denisov, V. M. Schreiber, *J. Mol. Struct.* **2001**, *560*, 151 – 159.

[17] S. Scheiner, *Hydrogen Bonding*, Oxford University Press, Oxford, NY, **1997**.

[18] a) N. V. Belkova, E. V. Bakhmutova, E. S. Shubina, C. Bianchini, M. Peruzzini, V. I. Bakhmutov, L. M. Epstein, *Eur. J. Inorg. Chem.* **2000**, 2163 – 2165; b) V. I. Bakhmutov, E. V. Bakhmutova, N. V. Belkova, L. M. Epstein, E. S. Shubina, E. V. Vorontsov, C. Bianchini, D. Masi, M. Peruzzini, F. Zanobini, *Can. J. Chem.* **2001**, *79*, 479 – 489.

[19] a) M. G. Basallote, J. Duran, M. J. Fernandez-Trujillo, M. A. Manez, J. R. Torre, *J. Chem. Soc. Dalton Trans.* **1998**, 745 – 749; b) M. G. Basallote, J. Duran, M. J. Fernandez-Trujillo, M. A. Manez, *J. Chem. Soc. Dalton Trans.* **1998**, 2205 – 2209.

[20] R. Cammi, R. Bonaccorsi, J. Tomasi, *Theor. Chim. Acta* **1985**, *68*, 271 – 283.

[21] F. B. van Duijnevelt, J. G. C. M. van Dijneveld-van de Rijdt, J. H. van Lenthe, *Chem. Rev.* **1994**, *94*, 1873 – 1885.

[22] F. Muguet, G. W. Robinson, *J. Chem. Phys.* **1995**, *102*, 3643 – 3654.

[23] F. Jensen, *Chem. Phys. Lett.* **1996**, *261*, 633 – 636.

[24] D. B. Cook, T. L. Sordo, J. A. Sordo, *J. Chem. Soc. Chem. Commun.* **1990**, 185 – 186.

[25] S. Simon, M. Duran, J. J. Dannenberg, *J. Chem. Phys.* **1997**, *105*, 11024 – 11031 and references therein.

Received: October 18, 2002 [F4510]